PHYSICAL REVIEW B

CONDENSED MATTER

THIRD SERIES, VOLUME 45, NUMBER 2 1 JANUARY 1992-II

Atomic-hydrogen concentrations in solid D-T and T_2

G. W. Collins, P. C. Souers, J. L. Maienschein, and E. R. Mapoles
Lawrence Livermore National Laboratory, Livermore, California 94550

J. R. Gaines
Department of Physics, University of Hawaii, Honolulu, Hawaii 96822
(Received 6 March 1991; revised manuscript received 8 August 1991)

We have measured the isothermal buildup of the atomic-hydrogen (T and D) concentration inside solid T_2 and D-T from 1.3 to 10 K. The atoms are produced by the β decay of tritium. Measurements were made using adiabatic slow-passage electron-spin-resonance (ESR) techniques. The atom concentration increases with time and does not saturate for the duration of our experiments (>2000 min). The atom concentration increases with decreasing temperature, and reaches values over 0.2% below 3 K. Using a simple analysis we find (1) the atomic recombination coefficients, (2) the production rate of trapped atoms that are visible with ESR, (3) the atomic diffusion coefficients, and (4) the trapping energy for atoms in the solid. Finally, we have observed that in D-T the number of D atoms is equal to the number of T atoms, while in HD+2%T_2 the number of H atoms is greater than the number of D atoms.

I. INTRODUCTION

In 1982 Kulsrud[1] discovered that the fusion reaction cross section for deuterium-tritium would increase by 50% if the nuclear spins are all polarized. This 50% improvement in the fusion cross section could allow a laser of perhaps half the originally contemplated power (and much lower cost) to be used. More[2] then calculated that compressional heating from a laser shot would not destroy the nuclear polarization before a nuclear reaction occurred. These two theoretical predictions were the foundation of our effort to spin-polarize DT. To date, we have studied the thermal conductivity and the triton nuclear magnetic resonance (NMR) in solid T_2 and D-T (a mixture composed of 25% D_2, 50% DT, and 25% T_2) from 2 K up to the triple point.[3-8] In this paper we report electron-spin-resonance (ESR) measurements of the atom concentration in solid T_2 and D-T, where the atoms are produced by the β decay of tritium. One scheme envisioned for polarizing the nuclei in DT uses the atoms in a dynamic polarization process.[9] One requirement for dynamic polarization is $(n/N)(T_{1n}/T_{1e}) \gg 1$, where n/N is the ratio of atoms to molecules, T_{1n} is the nuclear spin-lattice relaxation time of the molecules, and T_{1e} is the electron spin-lattice relaxation time of the atoms.[10] This paper characterizes (n/N) as a function of time and temperature.

This work is an extension of the work performed by Sharnoff and Pound.[11] They carefully measured the D-atom concentration inside D_2+1% T_2 using unmodulated, slow-passage ESR techniques at a resonance frequency of 24 GHz and at a temperature of 4.2 K. The deuterium atoms were produced from the β decay of tritium. The unsaturated signal that they detected contained two components, a narrow component and a broad line component. By multiplying the peak height by the full width at half the peak height, they obtained a "line strength" that was used to calculate the number of unpaired atoms. In plotting the "line strength," they saw a monotonic growth that saturated at about 200 min, followed by another period of growth with a second saturation at 8500 min. Based on the line shape and their observation of two different growth regions separated by a plateau, they concluded that there were two different types of atomic sites.

Leach and Fitzsimmons[12] measured the kinetics of H atoms in solid H_2. They bombarded solid H_2 with a beam of electrons from an accelerator where the beam current and pulse duration could be accurately controlled. After irradiating the sample with a given dose of radiation, they turned off the electron beam and observed the unpaired hydrogen atoms using ESR. They used adiabatic fast-passage techniques and recorded the dispersion component of the ESR signal as a function of time after irradiation. This experiment was repeated at several different temperatures. The dispersion signal they observed during fast passage, traced out, to a good approximation, the absorption component of the unsaturated signal. They related the product of the peak height and the linewidth to the number of spins. In doing so, they determined that the decay of the atomic hydrogen concentration, n, fol-

lowed a biatomic recombination process which could be described by the equation

$$dn/dt = -\alpha n^2 , \quad (1)$$

where α is the recombination coefficient and t is time. They found that in the temperature range 6.75–8.04 K, the recombination coefficient was described by $\alpha = \alpha_0 \exp(-E_a/k_B T)$, where the constants $\alpha_0 = 4.1 \times 10^{-14}$ m^3/s and $E_a/k_B = 195$ K, where T is temperature and k_B is Boltzmann's constant. Below this temperature range they observed a recombination coefficient that is much greater than that obtained by extrapolating the 6.75–8.04-K data.

Recently there has been much work toward understanding the kinetics of H and D atoms in solid mixtures of D_2, H_2, and HD.[13] Shevtsov and coworkers condensed the products of a rf discharge, trapping H and D atoms in mixtures of H_2 and D_2. They measured an increase in the concentrations of H atoms over time, accompanied by a decrease of D atoms. They concluded that the quantum tunneling reaction $D + H_2 \rightarrow HD + H$ must be occurring. Miyazaki *et al.* irradiated mixtures of solid D_2, H_2, and HD with a ^{60}Co source to produce unpaired atoms. They then removed the source and monitored the relative populations of H and D atoms with time using ESR. In HD, the ratio of H to D atoms just after irradiation was 5. It was observed that the number of H atoms was constant with time for over 400 min, whereas the number of D atoms decreased exponentially with a time constant of 130 min. From this work, and the work of Shevtsov, Miyazaki concluded that the D-atom population in mixtures of H_2 and D_2 or in HD is determined by a first-order rate equation $D + HD \rightarrow D_2 + H$ or $D + H_2 \rightarrow HD + H$ as opposed to the second order equation $D + D \rightarrow D_2$ used by Leach and Fitzsimmons. The low-temperature chemical reaction that exchanges the D atom for a H atom occurs via a quantum tunneling process and was first observed in solid HD by Solem.[9] The reaction occurs because the heavier product molecule has a lower vibrational zero-point energy. It has been studied for several years in gas phase reactions,[14] and only recently in the solid phase.

II. EXPERIMENTAL DETAILS

The probe used in these experiments was constructed at our laboratory and contained a continuous flow 1.2-K refrigeration stage based on Delong's original design.[15] This allowed stable temperatures from 1.2 K to room temperature for extended periods. The refrigeration capacity was 2 mW at 1.2 K. The evaporator, pumped by a 26-cfm mechanical pump, also served as the microwave cavity. During most of these experiments, the liquid-helium level was kept below the baseplate of the microwave resonator so that minor fluctuations in the liquid-helium level would not cause large fluctuations in the cavity's microwave resonant frequency. This was done by adjusting the impedance of the capillary which allows a calibrated rate of liquid-helium flow from a large helium^{-4} reservoir to the evaporator. The value of the impedance, which was determined by trial and error, was 2.26×10^{11}/cm^3.

The ESR (X-band) spectrometer was also constructed in our laboratory and was operated at 9.4 GHz. For most of the experiments, a homodyne detection scheme was used to monitor the steady-state absorption as the magnetic field was swept through a particular resonance. To keep from saturating the signal during a measurement (for spin counting), the power was kept between 10 μW and 0.3 nW. The magnetic field was not modulated and the sweep rate of the magnetic field through resonance was slow enough to maintain adiabatic and slow-passage conditions.[16] To keep the signal from being saturated, when the magnetic field is not modulated, the value for the transverse magnetic field, H_1 ($\sim$40 nT), must satisfy $H_1^2 \gamma^2 T_1 t_2 \ll 1$, where γ is the gyromagnetic ratio of the electron (28 025 MHz/T), T_1 is the spin-lattice relaxation time of the electron ($\sim$0.1 s), and t_2 is the spin-spin relaxation time of the electron ($\sim 10^{-8}$ s). The condition for adiabaticity is $dH_0/dt < \gamma H_1^2$. In our experiments, $dH_0/dt \leq 0.06$ mT/s. Even though T_1 and t_2 changed with time, these conditions were met for all of the data presented here.

The method used for extracting the number of atoms from the microwave absorption is as follows. An uncalibrated ruby sleeve was placed onto our sample cell located in the middle of the cavity. Because the locations of the ESR lines of ruby are dependent on the orientation of the crystal with respect to the external magnetic field, the crystal could be oriented so as to have no resonances within the hyperfine split T lines. A calibrated sample of DPPH was placed in the sample position of the cell. Unsaturated resonances of both DPPH and ruby were collected with the same experimental setup. These resonances were integrated and reduced to an area thereby transferring the calibration of the DPPH to the ruby standard. Each hydrogen resonance was then compared to a ruby resonance, taken under exactly the same conditions, to obtain a calibrated spin count. The TE_{011} cavity used in these experiments had an unloaded Q of about 5000. The estimated error in determining the number of atoms was about 15–20 %. To determine the atom concentration (the ratio of atoms to molecules), the amount of sample condensed into the sample cell was required. We had no way of measuring this quantity precisely but we were careful to ensure that the sample followed the saturated vapor pressure curve, with respect to the sample cell temperature, during condensation of the sample. Therefore, the absolute atom concentration measurements may be off by as much as 50%, but the relative accuracy between runs should be better than 20%.

The sample temperatures listed in this paper were the sample-cell temperatures as measured by a germanium resistance thermometer. The thermometer was glued into a hole that was specially machined into the sapphire sample cell to provide a close fit to insure good thermal contact. The sapphire sample cell had the dimensions 5.09 mm o.d., 4.05 mm i.d., and the thermometer was separated from the sample space by a 12-mm solid sapphire plug. The average hydrogen sample size was 0.0022 mol, so that the length of sample in the sample cylinder was 3.2 mm. Using the thermal conductivity data from Ref. 5, we can calculate the average sample temperature

by the relation

$$T(\text{av.}) = T(\text{sensor}) + A_0 L^2/8K \ , \quad (2)$$

where L is the cell radius, K is the thermal conductivity, and A_0 is the tritium self-heating constant calculated from the half-life (100 000 W/m^3 in solid T_2). Equation (2) assumes a one-dimensional loss of heat outward to the sapphire walls. It is possible that the effective value of A_0, in the solid phase, is smaller than the value determined from the tritium half-life. This is because a significant fraction of the β decay energy may be stored in the lattice as atoms and other defects, and possibly even emitted as light.[17,18]

The gas analysis was performed by Garza using a Varian MAT Model CH5 magnetic sector mass spectrometer. The accuracy is 1–5 % for a given component in a mixture with the 1% figure applicable to the component with the highest concentration. The T_2 and D-T gases for these experiments were desorbed from palladium source vessels. The gas composition of each palladium bed, used to supply tritium, changed only slightly over the course of the experiments. The mass spectrometer result for the T_2 palladium bed was typically 2% HT, 1% DT, and 97% T_2. The mass spectrometer result for the D-T palladium bed was typically 1% HD, 1% HT, 24% D_2, 49% DT, and 25% T_2. A new gas mixture was prepared for each experiment at each temperature. For the single HD+2% T_2 experiment reported in this paper, 97% HD was mixed with 98% T_2 for about 5 min at room temperature and then condensed into the solid phase.

III. EXPERIMENTAL DATA

Figure 1 shows the ESR spectrum of D-T at 1.7 K. The middle D line is centered at $g=2$. The hyperfine splittings for the D triplet was 214 MHz between the low-field D line and the middle D line and 224 MHz between the middle D line and the high-field D line. Although the middle D line contained a small contribution from nonatom resonances, the concentration of these impurities was always far less than $\frac{1}{3}$ of the D-atom concentration, and added little uncertainty in the measurement of the hyperfine splitting. The hyperfine splitting for the T atom was 1532 MHz. These values are close to the values found by Sharnoff and Pound.[11] They found the hyperfine splittings for the D triplet to be 201 MHz between the low-field D line and the middle D line and 237 MHz between the middle D line and the high-field D line. The hyperfine splitting observed for the T atom was 1517 MHz.

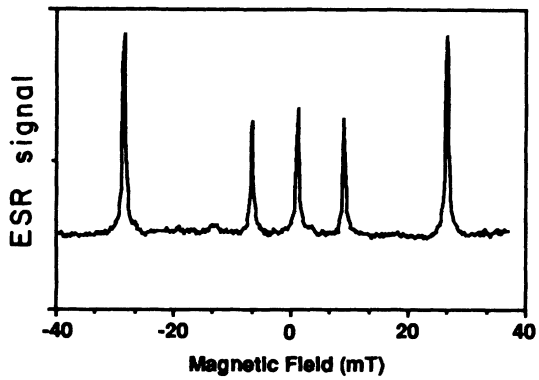

FIG. 1. ESR spectrum of D and T atoms in solid D-T at 1.7 K. The two larger outside lines are from the hyperfine spectrum of T atoms and the three middle lines are from the hyperfine spectrum of D atoms.

The isothermal buildup of the atom concentration in solid T_2 and D-T at several temperatures between 2 and 10 K is listed as a function of time in Tables I and II. Each sample was condensed from the gas phase and then slowly cooled to the temperature of the particular experiment. We then measured the ESR signal intensity for each of the hyperfine split atomic hydrogen lines while keeping a record of the time. These signal intensities were converted into an atom concentration using the calibration procedure described in the previous section. All the atom densities reported in this paper are listed in units of parts per million (ppm). The unit of ppm expresses the ratio of the number of atoms to the number of molecules (multiplied by 10^6) which is obtained from the sample volume and the molar volume. We used the extrapolated 0-K molar volumes[19] of 51 800 in D-T mol/m^3 and 53 000 mol/m^3 in T_2.

Figure 2 shows the total T-atom concentration versus time in solid T_2 at several temperatures. This figure illus-

TABLE I. The tritium atom concentration (ppm) versus time (min) inside solid T_2.

Time (min) 5.1 K	Atoms (ppm)	Time (min) 6.3 K	Atoms (ppm)	Time (min) 8.1 K	Atoms (ppm)	Time (min) 10.1 K	Atoms (ppm)
6	49	4	53	7	34	5	17
11	92	10	65	14	33	16	20
18	103	20	66	32	36	32	20
40	139	31	80	45	43	42	22
134	197	150	119	137	57	61	24
223	153	236	121	160	57	76	25
338	198	377	138	217	58	92	27
398	220	494	150	307	56	335	39
452	227	892	173	505	60	534	42
724	268	1028	185	764	67	734	51
1228	343	1263	191	1201	76	931	67

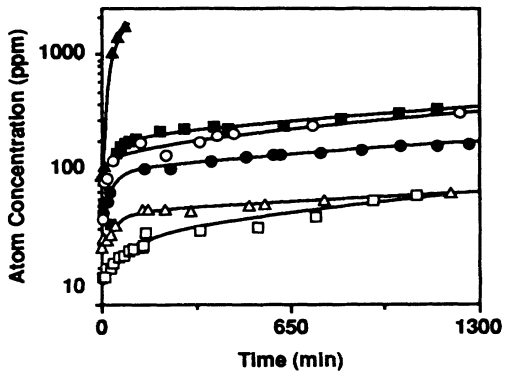

FIG. 2. Tritium atom concentration, [T], vs time in solid T_2 at the temperatures 2.1 (▲), 4.0 (■), 5.1 (○), 6.3 (●), 8.1 (△), and 10.1 K (□). The solid lines passing through the data points are from least-squares fits to the atom buildup data using Eq. (5). The parameters obtained from the fits are listed in Table III.

trates the general time-dependent behavior of the atom concentration in both T_2 and D-T. The atom concentration rapidly increases for the first 300 min. After this initial period, the rate of atom buildup slows to a finite and relatively constant value. Figure 2 also shows a rapid increase in atom density with decreasing temperatures. Table I lists the T-atom concentration in T_2 versus time at several temperatures.

Table II lists the D- and T-atom concentration versus time in D-T. We have listed separately the integrated intensity of the middle D line and the ratio [D]/[T]. We find the D-atom concentration, [D], is about equal to the T-atom concentration, [T], in D-T at all temperatures measured. It is difficult to make a meaningful comparison of the ratio [D]/[T] to previous experiments, since our measurements are made *during* sample irradiation. To compare the ratio [D]/[T] to the ratio [H]/[D] in HD, when measurements are made during irradiation, we have measured [H] and [D] in HD+2% T_2. In HD+2% T_2, [H] is greater than [D] by over a factor of 2. In Fig. 3 we

TABLE II. Atomic hydrogen concentration (ppm) versus time (min) in solid D-T. The total number of D atoms is calculated by multiplying the atom density of the high-field D line by three. The total number of T atoms is calculated by multiplying the atom density of the high-field T line by two. "Ratio Light-to-Heavy" is the ratio of D atoms to T atoms.

Temp. (K)	Time (min)	Total T atoms (ppm)	Total D atoms (ppm)	Atoms from middle D (ppm)	Total atoms (ppm)	Ratio Light-to-Heavy atoms
3.0 K	0	54	91	50	145	0.5
	36	151	132	54	283	1.1
	200	212	187	71	399	1.1
	289	231	192	84	423	1.1
	355	234	198	89	432	1.1
	531	238	188	91	426	1.1
	1215	240	211	91	451	1.0
4.0 K	13	56	48	25	104	1.0
	28	67	61		128	1.0
	54	82	72	29	154	1.0
	110	115	95	34	210	1.0
	159	132	133	50	265	0.9
	217	146	144		290	0.9
	1010	171	136	61	307	1.1
	1450	197	163	70	360	1.8
	2511	193	150	62	343	1.9
5.1 K	2	71	34	21	105	1.6
	33	82	43	25	125	1.5
	69	94	61	27	155	1.4
	189	95	73	40	168	1.1
	372	98	113	56	211	0.8
	1039	111	134	57	245	0.8
6.3 K	51	26	14	20	40	0.9
	125	40	24	25	64	1.0
	422	57	45	26	102	1.0
	1126	73	51	28	124	1.2
	2459	94	80	38	174	1.0

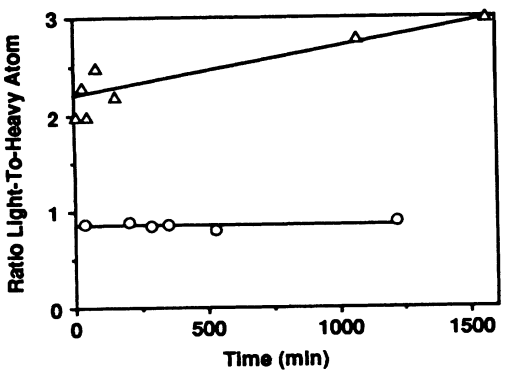

FIG. 3. The ratio of light to heavy atoms: [H]/[D] in HD+2% T_2 at 1.5 K (△) and [D]/[T] in D-T at 2.8 K (○) vs time. This shows that quantum tunneling is observed in HD but not D-T.

plot the ratio of the concentration of light atoms to heavy atoms for both D-T at 2.8 K and HD+2% T_2, at 1.5 K. As mentioned in the Introduction, the difference in the number of H atoms and D atoms is presumed to be due to low-temperature chemical reactions. Such reactions should be less effective in D-T than in H-D because the relative change in zero-point vibration energy for the reactions, $T+D_2\rightarrow DT+D$ and $T+DT\rightarrow T_2+D$, is less than the relative change in zero-point vibration energy for the reactions, $H_2+D\rightarrow HD+H$ or $HD+D\rightarrow D_2+H$, but it is somewhat surprising that we see no difference in the number of D and T atoms at all. We will present a detailed description of this low-temperature chemical reaction in tritiated hydrogen in a future publication.

The integrated signal intensities for both the high-field and low-field ESR transitions for the hyperfine multiplet of D or T were found to be essentially the same. It was therefore convenient to determine the total T-atom concentration by multiplying the area of the high-field peak by a factor 2. The middle line for deuterium was observed to be slightly larger than the two outer hyperfine D lines, presumably due to other paramagnetic species in the samples with an ESR transition near $g=2$. Accordingly, the total D-atom concentration was obtained by multiplying the area of the high-field line by three. We also estimated the number of nonatom spin-$\frac{1}{2}$ paramagnets centered at $g=2$ by subtracting the area of the high-field line from that of the middle D line. The nonatom concentration of $g=2$ spins varies up to 30 ppm.

IV. ANALYSIS

All of our ESR signals correspond to the narrow lines observed by Sharnoff and Pound.[11] We did not see the broad ESR lines that they reported. The time evolution of the atom concentration that we have measured is far from smooth, and, in addition, does not have the pronounced plateau of the Sharnoff and Pound data. Although the structure in the atom buildup curves may contain information on the different trapping sites, in this paper we analyze the curves by fitting them to a smooth function. This smooth function is obtained from a simple macroscopic model discussed below. While this model is neither rigorous nor complete, it serves as a first attempt at understanding these irradiated quantum crystals.

We first consider a crystal of solid hydrogen grown with some care as to have only a few cracks and a thermal equilibrium number of trapping sites. A β decay in a perfect hydrogen lattice would produce extensive local rearrangements of the molecules, as well as create many ion pairs and molecular fragments that eventually result in many unpaired atoms. In the solid, it is reasonable to assume that the unpaired atom concentration should increase until recombination with other atoms balances atom production. Assuming the concentration is homogeneous (fast-diffusion limit), the time dependence of the atom concentration is described by

$$\frac{dn(t)}{dt}=k-\alpha[n(t)]^2 , \tag{3}$$

where k is the production rate constant for all atoms produced by the decay of tritium, α is the atomic recombination coefficient, and $n(t)$ is the number of atoms per unit volume. An equilibrium atom density can be defined at steady state as $n(\text{eq.})=\sqrt{k/\alpha}$ and the time constant is defined as $\tau=1/\sqrt{k\alpha}$. If there are no atoms at $t=0$, this equation has the simple solution

$$n(t)=n(\text{eq.})\tanh(t/\tau) , \tag{4}$$

where $n(t)$ initially grows linearly and then saturates. The atom concentration we measure does not simply saturate as predicted by the above equation but continues to increase with time. We fit the atom buildup curves to the equation

$$n(t)=n(\text{eq.})\tanh[(t-t_0)/\tau]+c(t-t_0) , \tag{5}$$

where $n(\text{eq.})$, τ, c, and t_0 are the adjustable parameters. c empirically takes into account the nonsaturating behavior of the atom concentration, and t_0 shifts the time axis to take into account the concentration of atoms that exist when the experiment begins due to the finite time it takes to cool the apparatus to a set temperature. We can consider the nonsaturating part of Eq. (5) to be a small perturbation of Eq. (4). The quantities $n(\text{eq.})$, α, k, and c, derived from the fits are listed in Table III. Examples of the fits for the T_2 data are shown as solid lines going through the experimental data points in Fig. 2.

From Table III we notice that t_0 is small at the lower temperatures and increases for higher sample temperatures. This results from the finite time it takes to cool the sample, combined with the strong temperature dependence of the atom concentration. This is most clearly illustrated by the data at 10 K where the atom buildup curve does not have the early transient buildup because the atom density is already equilibrated by the time our measurements begin. At lower temperatures, the equilibrium atom density is higher. This means that, at the lower temperatures, most of the atoms are still to be produced by the time we reach the desired temperature, and the shift of the time axis is less relevant than at the higher temperatures.

In Fig. 4, the values for the recombination coefficients

TABLE III. Parameters found from fitting our model summarized by Eq. (5) to the atom buildup data. The derived quantities are explained in the text. The numbers in parentheses are powers of ten. D is the atom diffusion coefficient.

	Temp. (K)	n(eq.) (ppm)	t_0 (min)	m (ppm/min)	α (m^3/s)	k (1/m^3 s)	k/k(gas)	D (m^2/s)
T in T_2	2.1	3458	0		1(−30)	1(22)	1(−1)	2(−22)
	4.0	200	5	0.14	5(−29)	2(21)	2(−2)	1(−20)
	5.1	151	2	0.16	1(−28)	3(21)	3(−2)	3(−20)
	6.3	112	26	0.07	7(−29)	9(20)	1(−2)	2(−20)
	8.1	52	60	0.02	1(−28)	3(20)	3(−3)	2(−20)
	10.1	25	70	0.04	2(−28)	1(20)	2(−3)	5(−20)
D+T in DT	2.2	1754	7	2.88	8(−30)	2(22)	5(−1)	2(−21)
	3.0	406	21	0.04	2(−29)	3(21)	7(−2)	4(−21)
	4.0	318	53	0.01	8(−30)	8(20)	2(−2)	2(−21)
	5.1	178	135	0.06	1(−29)	4(20)	1(−2)	3(−21)
	6.3	86	27	0.04	3(−29)	2(20)	6(−3)	8(−21)

obtained from the fits to our data (listed in Table III) and from previous data for H atoms[12] in H_2 and D atoms[20] in D_2 are plotted as a function of inverse temperature. Figure 4 shows that our values for the recombination coefficients are much larger than the values found from previous experiments. We believe this difference is due to the large amount of radiation damage in our samples as compared to the samples of the previous experiments.

A diffusion coefficient, D, can be related to the recombination coefficient, α, by the expression[21]

$$D=\alpha/4\pi R_0 , \tag{6}$$

where R_0 is on the order of the lattice constant. In this simple kinetic equation we have set the radius of the geometric cross section and the mean free path equal to the intermolecular distance. The calculated diffusion coefficients from Eq. (6) are listed in Table III and plotted versus inverse temperature in Fig. 5. To establish the validity in using Eq. (6) for determining the atomic diffusion coefficient, we will compare them below with (1) the atomic diffusion coefficients derived from the molecular $J=1$ to $J=0$ conversion of homonuclear molecules in T_2 and D-T, and (2) the molecular diffusion coefficients in the solid, a few degrees below the triple point.

The $J=1$ to $J=0$ conversion of T_2 and D_2 molecules in T_2 and D-T is catalyzed by the unpaired hydrogen atoms. If the atom concentration is known, we can calculate an atomic diffusion coefficient from the time constant of the exponential decay of the $J=1$ molecules. The diffusion coefficients from the $J=1$ to $J=0$ conversion have been calculated in Ref. 8 and are plotted in Fig. 5. The diffusion coefficients calculated from the $J=1$ to $J=0$ conversion are very close to the values of the atomic diffusion coefficient calculated from the recombination coefficient.

It has been shown that, in the high-temperature solid, i.e., a few degrees below the triple point, the diffusion for H_2, D_2, D-T, and T_2 molecules is thermally activated and fits the vacancy hopping model of Ebner and Sung.[22] Leach[12] has measured the recombination of H in H_2, and Iskovskikh *et al.*[20] have measured the recombination of

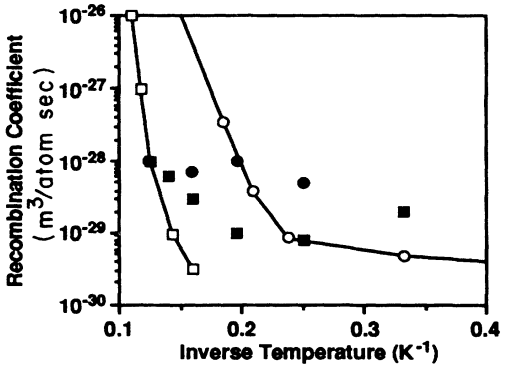

FIG. 4. The atom recombination coefficient, α, vs inverse temperature for some of the work presented here, T_2 (●), D-T (■), and previous reports studying H atoms in H_2 (Ref. 12) (○) and D atoms in D_2 (Ref. 20) (□).

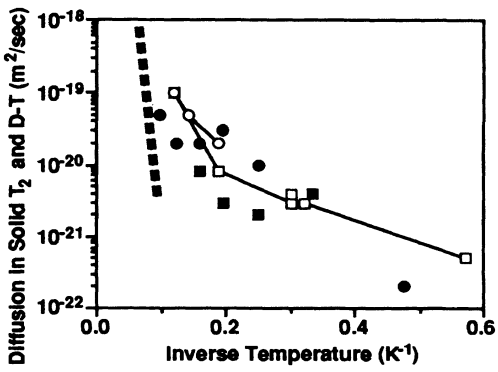

FIG. 5. Diffusion coefficients in solid hydrogen vs inverse temperature: (a) atomic diffusion coefficients in T_2 (●) and D-T (■) calculated from Eq. (6), (b) atomic diffusion coefficients in T_2 (○) and D-T (□) derived from the analysis of the $J=1$ to $J=0$ conversion (Ref. 8), (c) the bold dashed line represents the extrapolated value of the molecular diffusion coefficient from nuclear magnetic resonance studies of the molecules (Ref. 4) in T_2 and D-T.

D atoms in D_2. The diffusion coefficient they calculate from the recombination coefficient in the high-temperature solid has the same activation energy as that measured for the molecules; namely, 195 K for H atoms in H_2 between the temperatures 6.75 and 8.04 K and 270 K for D atoms in D_2 between the temperatures 7.5 and 9.5 K. Iskovskikh *et al.*[20] have also measured the recombination of H atoms in H_2, and between the temperatures 4.8 and 5.4 K they obtained an activation energy of 103 K. The large difference between the two activation energies measured for H atoms in H_2 could be an error caused by the narrow temperature ranges used in the two different experiments. One interesting observation is that, while the activation energy measured by Leach is very close to that calculated by Ebner and Sung for the high-temperature "classical" diffusion of the molecules, the activation energy measured by Iskovskikh *et al.* is close to the activation energy also calculated by Ebner and Sung for the low-temperature "quantum" diffusion regime.

The prefactor for the diffusion coefficient was different for the atoms[12,20] and molecules[22–24] but the lattice was also much more damaged from the production of atoms inside the solid. None of our measurements were in the high-temperature solid, but at our highest temperatures, the diffusion coefficient, as measured by recombination [Eq. (6)], appears to be converging to the value from the molecular diffusion measurements in the high-temperature solid. The molecular diffusion coefficient in the high-temperature solid in T_2 and D-T has been measured by standard NMR techniques.[3] We have extrapolated the values of the molecular diffusion coefficient to lower temperatures and plotted this extrapolation in Fig. 5, along with the diffusion coefficients derived from the recombination coefficient and the $J=1$ to $J=0$ conversion in D-T and T_2.

We next turn to the rate constant, k, defined in Eq. (3). This constant characterizes the rate at which atoms are produced by tritium decay. The triton has a half-life of 12.3 yrs (Ref. 25) and undergoes a β decay with a mean energy of 5.69 keV.[26] The β particle looses its kinetic energy as it collides with the electron clouds of hydrogen molecules. There is an energy loss of 36.6 eV per ion pair, leading to 155 ion pairs (in the gas) for the average energy β particle. Previous estimates from gas phase kinetics imply that 780 unpaired atoms are formed per triton decay or about 5 atoms per ion pair.[27] The atom production rate, k(gas), from gas-phase data, can be written as[28,29]

$$k(\text{gas})=3.4\times10^{17}\rho f_T A \ , \tag{7}$$

where ρ is the density (mol/m^3), f_T is the atomic fraction of tritium, A is the number of atoms produced per ion pair (five for the gas phase), and 3.4×10^{17} is the number of ion pairs produced per mole second in tritium.

Although most of the energy-loss data for electrons in hydrogen is from the gas phase, Schou and Sorensen bombarded solid H_2 and D_2 with 500–3000 eV electrons[30] and found the β particle range in the solid scaled with density the same as in the gas. Using the gas-phase equation [Eq. (7)] for the production rate of atomic hydrogen in the solid phase, where the molar volume is about 50 000 mol/m^3, the β particle creates an ion pair and excites one molecule every 100 lattice spacings for about 3 μm. The molecular excitations create on the average one atom every 100 lattice spacings. The molecular ionization creates one atom directly when it recombines with another molecule to form $H_3^+ + H$. In the gas phase, the ion pair creates three more atoms upon electron recombination with H_3^+. In the solid, the surrounding molecules could take up the extra energy, and thus only two atoms might be formed per molecular ion. There is one estimate for the production of atoms in the solid phase that implies over 1000 unpaired atoms are formed per triton decay.[3] More recently, we have measured an exchange time for the reaction, $2DT \leftrightarrow D_2 + T_2$, of 200 h in solid phase at 6 K.[8] As shown in Ref. 8, this suggests that the number of atoms produced in the solid phase is the same as in the gas phase.

When we use the gas-phase equation [Eq. (7)] to calculate the production rate of atomic hydrogen in solid T_2, we find

$$k(\text{gas})=9.0\times10^{22} \text{ atoms m}^{-3}\text{s}^{-1} \ . \tag{8}$$

When we compare this result to the values of k obtained from our data, we find

$$k \ll k(\text{gas}) \ . \tag{9}$$

In Table III we list the values for the rate constant k and the ratio k/k(gas). From Table III we also see that there is a temperature dependance in the value of k. Although the temperature dependence of k is not a perfect exponential, we can fit the four warmest data points for both T_2 and D-T to the function

$$k=k_0\exp(-E_a/k_BT) \ , \tag{10}$$

where k_0 is a constant and E_a is the trapping energy for the atoms. We find E_a/k_B is 33 K in T_2 and 14.5 K in D-T. This implies that the atoms measured in our ESR experiments are trapped in sites with an energy on the order of 33 K in T_2 and 14.5 K in D-T. This agrees fairly well with the trapping energy calculated by Danilowitz and Etters[31] of 15.9 K for H atoms in H_2.

The large discrepancy between our value of k and k(gas) can be either due to (1) atoms that are formed close together, do not recombine rapidly, but cannot be detected by our present method of observation, or (2) atoms that are formed close together and recombine rapidly. Suggestion (1) implies that there may be a large fraction of atoms in the solid not detected by our present experimental technique. Suggestion (2) implies that the atoms produced close together recombine so rapidly that the number of atoms with nearby neighbors is much smaller than the number of atoms we see with ESR. At the present time we cannot decide between suggestions (1) or (2). The reason our present experimental technique can-

not detect any atom that is within about three lattice spacings from another atom is because the magnetic field around an atom is shifted 35.2, 4.4, and 1.4 mT for a distance of 1, 2, and 3 lattice spacings, respectively. This shifts the resonant frequency of an atom outside our ESR window. The ESR integration window was set at five times the linewidth and the linewidth ranged from 0.1 to 0.6 mT.[32] Thus, two atoms that were within two to three lattice spacings from each other were not detected. For an atom to be "produced," it must diffuse at least three lattice spacings from a near atom without recombining.

ACKNOWLEDGMENTS

We would like to thank Chris Gatrousis and Tom Sugihara of the Chemistry and Materials Science Department, Erik Storm of the Inertial Confinement Fusion Program, and John Holzrichter and John Nuckolls of the Institutional Research and Development Program, all of LLNL, for their support of this work. Work performed under the auspices of the U.S. Department of Energy by the Lawrence Livermore National Laboratory under Contract No. W-7405-ENG-48.

[1]R. M. Kulsrud, H. P. Furth, E. J. Valeo, and M. Goldhaber, Phys. Rev. Lett. **49**, 1248 (1982).

[2]R. M. More, Phys. Rev. Lett. **51**, 396 (1983).

[3]J. D. Sater, J. R. Gaines, E. M. Fearon, P. C. Souers, F. McMurphy, and E. R. Mapoles, Phys. Rev. B **37**, 1482 (1988).

[4]J. R. Gaines, P. C. Souers, E. M. Fearon, J. D. Sater, and E. R. Mapoles, Phys. Rev. B **39**, 3943 (1989).

[5]G. W. Collins, P. C. Souers, E. M. Fearon, E. R. Mapoles, R. T. Tsugawa, and J. R. Gaines, Phys. Rev. B **41**, 1816 (1990).

[6]P. C. Souers, E. M. Fearon, E. R. Mapoles, J. D. Sater, G. W. Collins, J. R. Gaines, R. H. Sherman, and J. R. Bartlit, Fusion Tech. **14**, 855 (1988).

[7]E. M. Fearon, R. G. Garza, C. M. Griffith, S. R. Mayhugh, E. R. Mapoles, P. C. Souers, R. T. Tsugawa, J. D. Sater, G. W. Collins, and J. R. Gaines, Fusion Tech. **14**, 864 (1988).

[8]G. W. Collins, E. M. Fearon, E. R. Mapoles, P. C. Souers, and P. A. Fedders, Phys. Rev. B **44**, 6598 (1991).

[9]J. C. Solem and G. A. Rebka, Jr., Phys. Rev. Lett. **21**, 19 (1968); J. C. Solem, Nucl. Instrum. Methods **117**, 477 (1974).

[10]A. Abragam and M. Goldman, *Nuclear Magnetism: Order and Disorder* (Clarendon, New York, 1982), p. 341.

[11]M. Sharnoff and R. V. Pound, Phys. Rev. **132**, 1003 (1963).

[12]R. Leach, Ph.D. thesis, University of Wisconsin, University Microfilms, Ann Arbor, MI, 1972.

[13]A. V. Ivliev, A. S. Iskovskikh, A. Ya. Katunin, I. I. Lukashevich, V. V. Sklyarevskii, V. V. Suraev, V. V. Filippov, N. I. Filippov, and V. A. Shevtsov, Pis'ma Zh. Eksp. Teor. Fiz. **38**, 317 (1983) [JETP Lett. **38**, 379 (1983)]; T. Miyazaki, N. Iwata, K. Lee, and K. Fueki, J. Phys. Chem. **93**, 3352 (1989), and references within.

[14]E. F. Caldin, Chem. Rev. **69**, 135 (1969).

[15]L. E. Delong, O. G. Symko, and J. C. Wheatley, Rev. Sci. Instrum. **42**, 147 (1971).

[16]C. P. Poole, *Electron Spin Resonance,* 2nd ed. (Wiley, New York, 1983), Chap. 13.

[17]G. W. Collins, E. M. Fearon, E. R. Mapoles, P. C. Souers, and J. R. Gaines, Phys. Rev. Lett. **65**, 444 (1990).

[18]E. R. Mapoles, F. Magnotta, G. W. Collins, and P. C. Souers, Phys. Rev. B **41**, 11 653 (1990).

[19]P. C. Souers, *Hydrogen Properties for Fusion Energy* (University of California, Berkeley, 1986), p. 80.

[20]A. S. Iskovskikh, A. Ya. Katunin, I. I. Lukashevich, V. V. Sklyarevskii, V. V. Suraev, V. V. Filippov, M. I. Filippov, and V. A. Shevtsov, Zh. Eksp. Teor. Fiz. **91**, 1832 (1986) [Sov. Phys. JETP **64**, 1085 (1986)].

[21]Sidney W. Benson, *The Foundations of Chemical Kinetics* (McGraw-Hill, New York, 1960), Chap. 15.

[22]C. Ebner and C. C. Sung, Phys. Rev. A **5**, 2625 (1971).

[23]F. Weinhaus, H. Meyer, S. M. Myers, and A. B. Harris, Phys. Rev. B **7**, 2960 (1973).

[24]M. Bloom, Physica **23**, 767 (1957).

[25]C. R. Rudy and K. C. Jordan (unpublished).

[26]W. L. Pillinger, J. J. Hentges, and J. A. Blair, Phys. Rev. **121**, 232 (1961).

[27]W. M. Jones and D. F. Dever, J. Chem. Phys. **60**, 2900 (1974).

[28]D. Combecher, Radiat. Res. **84**, 189 (1980).

[29]G. N. Whyte, Radiat. Res. **18**, 265 (1963).

[30]J. Schou and H. Sorenson, J. Appl. Phys. **49**, 816 (1978).

[31]R. L. Danilowicz and R. D. Etters, Phys. Rev. B **19**, 2321 (1979).

[32]This linewidth data implies that the number of atoms missed with our present technique of counting is over an order of magnitude in aged samples.